scientific reports

OPEN

Evaluating the influence of land use and land cover change on fine particulate matter

Wei Yang[1]✉ & Xiaoli Jiang[2]

Fine particulate matter (i.e. particles with diameters smaller than 2.5 microns, $PM_{2.5}$) has become a critical environmental issue in China. Land use and land cover (LULC) is recognized as one of the most important influence factors, however very fewer investigations have focused on the impact of LULC on $PM_{2.5}$. The influences of different LULC types and different land use and land cover change (LULCC) types on $PM_{2.5}$ are discussed. A geographically weighted regression model is used for the general analysis, and a spatial analysis method based on the geographic information system is used for a detailed analysis. The results show that LULCC has a stable influence on $PM_{2.5}$ concentration. For different LULC types, construction lands have the highest $PM_{2.5}$ concentration and woodlands have the lowest. The order of $PM_{2.5}$ concentration for the different LULC types is: construction lands > unused lands > water > farmlands >grasslands > woodlands. For different LULCC types, when high-grade land types are converted to low-grade types, the $PM_{2.5}$ concentration decreases; otherwise, the $PM_{2.5}$ concentration increases. The result of this study can provide a decision basis for regional environmental protection and regional ecological security agencies.

With the rapid development of China's economy and society, its rate of urbanization is accelerating. China's industrial scale is also expanding rapidly, and the problem of air pollution is becoming increasingly serious, which has a tremendous impact on the environment, economic development, and even people's health[1]. Fine particulate matter (i.e. particles with diameters smaller than 2.5 microns, $PM_{2.5}$) is considered a crucial protagonist among the various air pollution factors[2]. As a significant health hazard, $PM_{2.5}$ is highly associated with an increased probability of respiratory diseases[3,4], cardiorespiratory problems[5,6], mutagenic diseases[7] and increased mortality. Therefore, it is of vital significance to understand $PM_{2.5}$ pollution clearly, especially its distribution characteristics and influence factors, which are helpful for reducing pollution and protecting human health.

As a severe air pollutant, the concentration of $PM_{2.5}$ is influenced by meteorological factors[8–10], human activities[11], and the surrounding environment[12]. $PM_{2.5}$ is emitted mainly from anthropogenic sources, such as from traffic[13] and industrial production[14]. The spatial and temporal distributions of $PM_{2.5}$ are impacted by meteorological and environment factors[15–17]. Previous research has revealed that $PM_{2.5}$ is severely affected by meteorological factors at the macro-scale[18] in terms of temperature[19], precipitation[20], wind conditions[21,22], etc., while at the micro-scale, $PM_{2.5}$ is strongly associated with land use and land cover (LULC) type[23]. Optimizing LULC type may reduce $PM_{2.5}$ pollution at the community or city level[24,25]. Land use and land cover change (LULCC) is the embodiment of human activities, which also has an obvious effect on $PM_{2.5}$ distribution[26]. To mitigate pollution, it is significant to explore the effects of LULC and LULCC on $PM_{2.5}$ pollution.

To conduct research on the relationship between LULCC and $PM_{2.5}$, relevant data are required. Remote sensing based LULCC research has a long history and is relatively mature[27,28], which has become an effective method to obtain LULCC data. Conventional methods of obtaining $PM_{2.5}$ data employ monitoring stations at fixed sites, whose effective monitoring distances range from 0.5 to 4 km[29], and which can provide accurate point-source data. The area among the monitoring sites can not been represented by this data. Due to the discontinuous spatial distribution of sites monitoring $PM_{2.5}$ data, several methods have been employed to solve this problem, including spatial interpolation[30], chemical transport models[31], land-use regression models[32] and aerosol optical depth (AOD) based statistical models[33]. However, as the use of a single approach leads to large uncertainties, some researchers have sought to integrate different methods to improve the $PM_{2.5}$ estimation accuracy, such as a combination of chemical transport models and satellite-derived AOD[34,35].

[1]School of Geography Science, Taiyuan Normal University, Daxue street, Yuci district, Jinzhong 030619, Shanxi, China. [2]Research Center for Scientific Development in Fenhe River Valley, Taiyuan Normal University, Jinzhong 030619, Shanxi, China. ✉email: weiaiweiwei@163.com

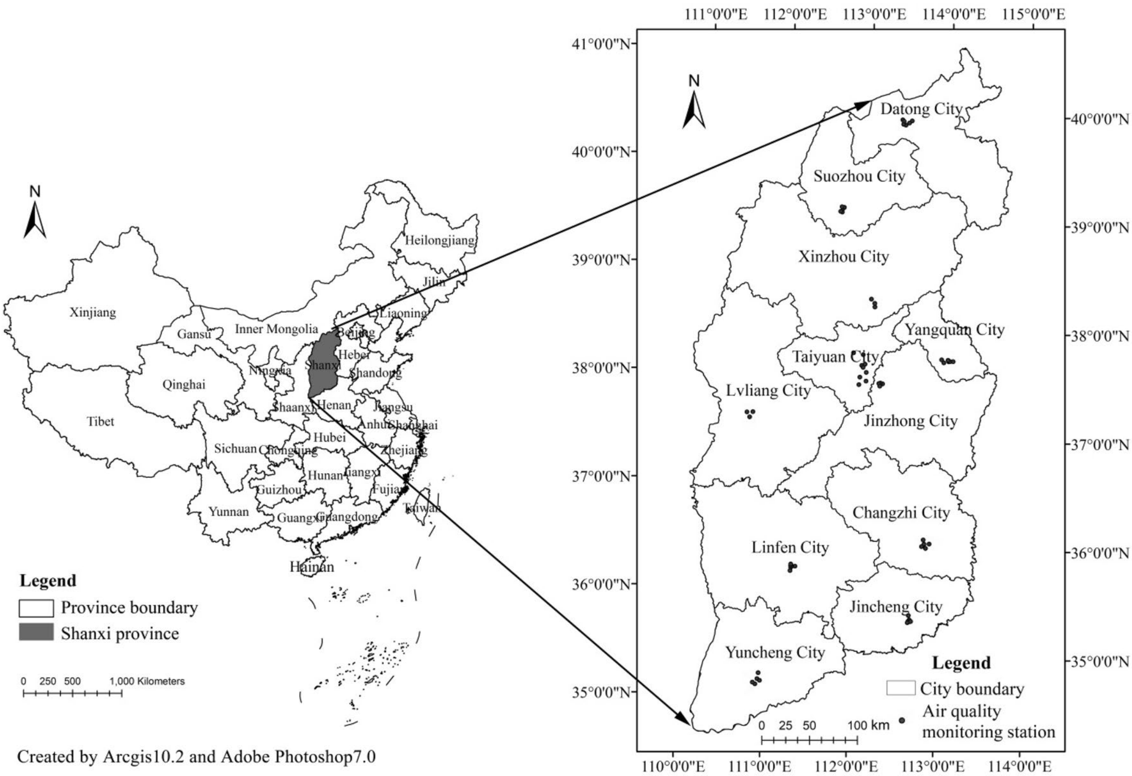

Figure 1. The location of Shanxi Province in China and the location of air quality monitoring stations in Shanxi Province.

At present, researches on the relationship between $PM_{2.5}$ and land use mostly focus on city scale[36,37]. Due to atmospheric transport, $PM_{2.5}$ distribution is not only affected by local emissions, but also regional transport[38]. Regional land use changes can directly or indirectly affect $PM_{2.5}$ distribution. There is an insufficient amount on research at regional scale. Moreover, most of the existed researches focus on the influence of landscape patterns on $PM_{2.5}$ pollution but not LULCC types[39,40]. And the $PM_{2.5}$ data used in these studies was station monitoring data which is spatially discontinuous and cannot reveal the spatial relationship between $PM_{2.5}$ and LULCC types. Therefore, in this paper we analyze the relationship between dynamic $PM_{2.5}$ and LULCC type. To avoid the spatial discontinuity of station monitoring $PM_{2.5}$ data, the spatially continuous $PM_{2.5}$ data from the Atmospheric Composition Analysis Group (ACAG) are used. A geographical weighted regression model and a spatial analysis method are employed to identify the response mechanism between dynamic $PM_{2.5}$ and LULCC type. The results of this study can provide a decision basis for regional environmental protection and regional ecological security agencies.

Methodology

Study area. Shanxi Province is located in the middle of China (Fig. 1), which is the most important energy bases in the country and whose coal output was ranked first before 2016, and second thereafter. Due to the abundance of coal resources in Shanxi Province, its energy structure is focused on coal, which accounts for 72% of its total energy consumption. Shanxi Province is not only an important coal exporter, but also an important power exporter. The power plants in Shanxi Province are mainly coal-fired, which produce considerable amounts of emissions. Additionally, coking and steel industries are pillar industries in Shanxi Province, which also produce vast amounts of emissions. This economic structure based on energy consumption causes serious air pollution. Several cities in Shanxi Province, such as Taiyuan, Linfen, Jincheng, etc., contain the worst air pollution of all cities in China. Meanwhile, Shanxi Province had experienced obvious LULCCs, such as urban expansion caused by fast urbanization and an increase of green land owing to the growth of the 'Grain for Green' project. Therefore, Shanxi Province was selected as the study area to analyze the relationship between LULCC and $PM_{2.5}$.

Data acquisition and preparation. *$PM_{2.5}$ data.* The $PM_{2.5}$ data provided by ACAG were generated based on a combination of a chemical transport model, satellite observations and ground-based observations[41]. The data have been validated in North America, which have been shown to have higher accuracy than purely geoscience-based estimates[35]. However, the accuracy of the ACAG data of China has not been validated; therefore, in this work we estimated its accuracy (see Sect. 3.1).

Ground-based data from 58 state-controlled air quality monitoring stations from 2018 were used in the validation (Fig. 1). The ACAG $PM_{2.5}$ data from 2000 to 2018 were downloaded from (http://fizz.phys.dal.ca/

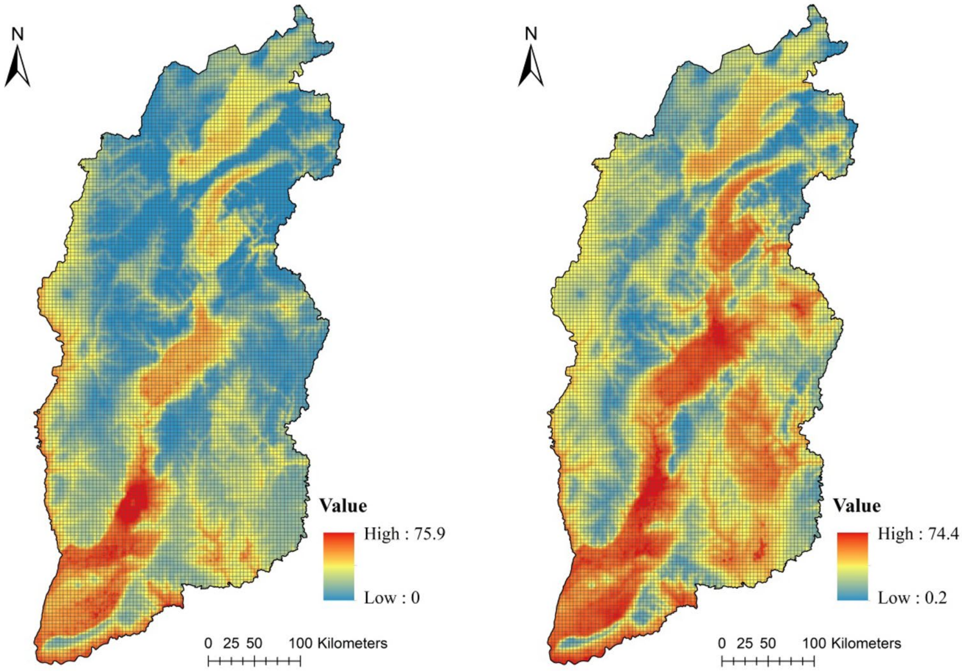

Figure 2. 3 × 3 km grid map and ACAG PM2.5 concentration data of Shanxi Province in 2000 and 2018 (units: μg/m^3).

~atmos/martin/?page_id=140%E3%80%822014). The initial data were reprojected and resampled to a 1-km spatial resolution (Fig. 2).

Pearson's correlation coefficient and the root mean square error (RMSE) were calculated in the validation as:

$$\text{Pearsoncorrelationcoefficient} = \frac{N\sum X_i Y_i - \sum X_i \sum Y_i}{\sqrt{N\sum X_i^2 - (\sum X_i)^2}\sqrt{N\sum Y_i^2 - (\sum Y_i)^2}} \tag{1}$$

$$\text{RMSE} = \sqrt{\frac{1}{n}\sum_{i=1}^{n}(X_i - Y_i)^2} \tag{2}$$

where X_i represents a $PM_{2.5}$ value from the ACAG, and Y_i represents a $PM_{2.5}$ value from monitoring stations.

Land use and land cover data. The China multi-period land use land cover data set (CNLUCC) was used. The CNLUCC data were generated with a visual interpretation method based on Landsat remote-sensing data. The data set was provided by the Data Center for Resources and Environmental Sciences, Chinese Academy of Science (http://www.resdc.cn). Data in 2000 and 2018 were used (Fig. 3). The data consist of six classes: farmlands, forests, grasslands, water, construction lands, and unused lands. The data were shown to have an accuracy of 88.95%, which meet the needs of this study.

Geographical weighted regression model. Geographical weighted regression (GWR) models are a powerful tool to explore the heterogeneity of spatial relations[42]. As a local spatial regression model, GWR can effectively solve the nonstationarity of variable space, which has been widely used in the spatial analyses of different geographic elements[43]. The essence of GWR is locally weighted least squares, where the 'weight' is a distance function of spatial position between the point to be estimated and other observation points. The expression of GWR is as follows:

$$y_i = a_0(u_i, v_i) + \sum_k a_k(u_i, v_i)x_{ik} + \varepsilon_i \tag{3}$$

where y is the dependent variable, x is the explanatory variable, (u_i, v_i) is the coordinates of the ith point in space, $a_k(u_i, v_i)$ is a realization of the continuous function $a_k(u, v)$ at point i, and ε_i is the error term.

To identify the spatial relationship between LULCC and $PM_{2.5}$, a 3 × 3 km grid map (Fig. 2) was generated of the study area. The variations of $PM_{2.5}$ between 2000 and 2018 were calculated in each grid, where the results were considered as the dependent variable in Eq. (3). The changing area of each different land type in each grid was also calculated and considered as the explanatory variable. Four main land types, farmlands, woodlands, grasslands

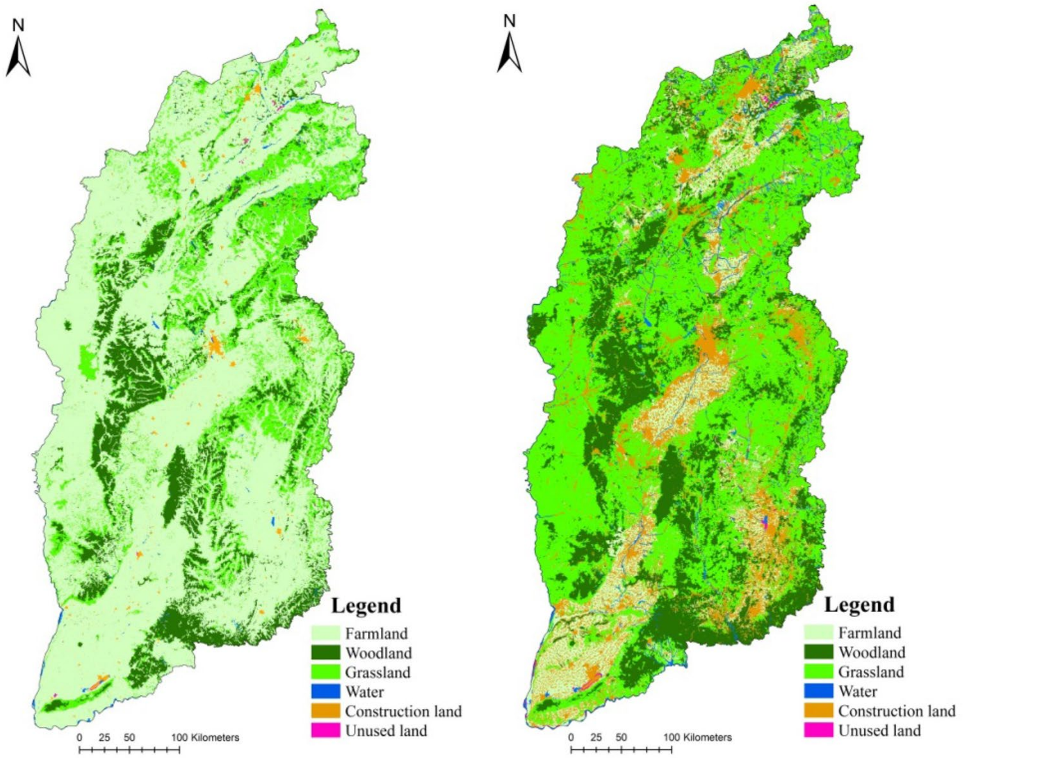

Figure 3. The land use and land cover data in 2000 and 2018.

and construction lands, were selected as the explanatory variables because their combined area accounted for nearly 99% of the total area.

Analysis framework. A GWR analysis was used to determine the overall characteristic between the LULCC and $PM_{2.5}$ dynamics. After that, based on the spatial analysis tools in ArcGIS 10.2, a detail analysis was conducted from two aspects: (1) $PM_{2.5}$ distributions for the different LULC types, and (2) $PM_{2.5}$ dynamics for the different LULCC types. The analysis process is shown in Fig. 4.

Results

Validation of the $PM_{2.5}$ data. As mentioned above, station monitoring data can represent a scope from 0.5 to 4 km. Thus, a 4-km buffer from each monitoring station was generated. In the buffer, the mean values of the $PM_{2.5}$ data from ACAG were calculated and validated according to the station monitoring data. The results (Table 1) show an RMSE of 7.05 and a Pearson's correlation coefficient of 0.82, which show that the ACAG $PM_{2.5}$ data have high consistency with the ground-based observational data.

GWR analysis. The GWR analysis showed that R^2 reached 0.94 which implies a good fitting effect. 93.56% of the standardized residuals were between − 2 and 2, which demonstrates that the model fitting was stable[44]. The results show that there was a stable relationship between $PM_{2.5}$ and LULCC. As shown in Fig. 5, the local R^2 values were between 0.01 and 0.93. In contrast with the LULCC data, the high values of the local R^2 were distributed in places where the LULCC showed an obvious dynamic while the low local R^2 values were distributed in LULCC areas that did not change. The result indicated that dynamic $PM_{2.5}$ had a significant response to LULCC.

Effect of the LULC type on $PM_{2.5}$. To further investigate the relationship between the $PM_{2.5}$ dynamics and the different LULC types, a spatial analyze based on ArcGIS was conducted. The results (Table 2) show that, for all LULC types, the mean $PM_{2.5}$ concentrations significantly increased from 2000 to 2018. Among them, unused lands had the largest increase. Woodlands and grasslands had the largest increasing rates, 86.02% and 81.00%, respectively. Construction lands had the lowest increasing rate of 20.92%. The rates of increase of other the LULC types were relatively close, with a scope of 38.45% and 47.99%. The increasing trends indicate that the $PM_{2.5}$ pollution situation worsened during the study period. The standard deviations (SDs) all increased, meaning that the spatial difference of $PM_{2.5}$ pollution was increased. Indeed, the whole study area is faced with a seriously $PM_{2.5}$ polluted situation.

Furthermore, for the different LULC types, in 2000, woodlands had the lowest mean $PM_{2.5}$ concentration, although that of the grasslands was very similar. Construction lands had the highest mean $PM_{2.5}$ concentration. In 2018, the mean $PM_{2.5}$ concentrations of the woodlands and grasslands were still very close, and were

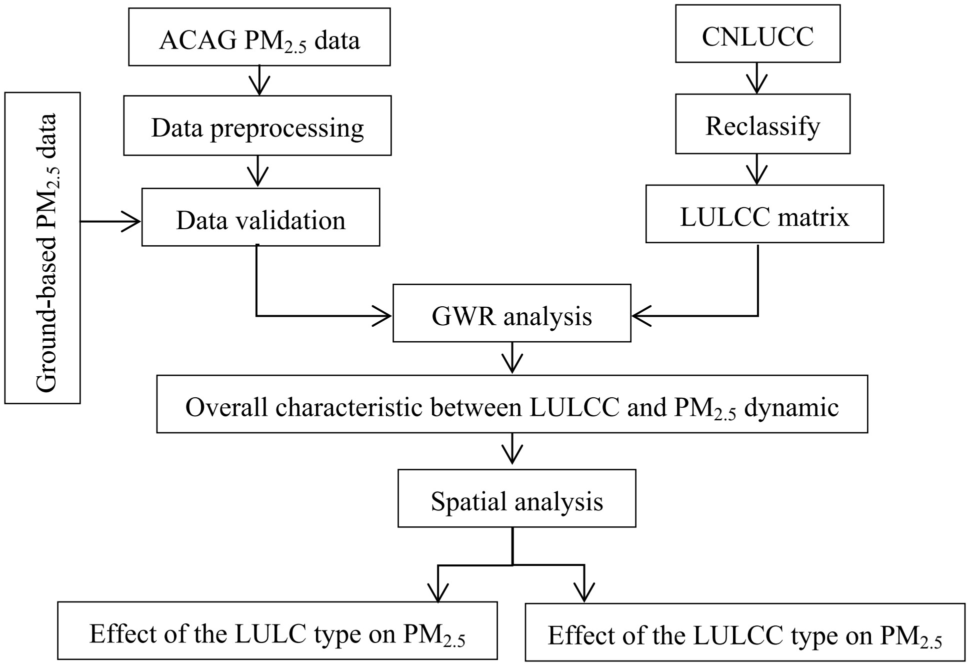

Figure 4. Analysis framework used in this study.

$PM_{2.5}$	Max	Min	Mean	SD	RMSE	Pearson correlation
Station monitoring	84.03	30.42	58.18	12.01	7.05	0.82
ACAG	74.40	32.20	59.78	11.19		

Table 1. Validation of the $PM_{2.5}$ data (units: μg/m[3]).

still the lowest values. The $PM_{2.5}$ concentration of the construction lands was still the highest. In both 2 years, the order of $PM_{2.5}$ concentration for the different LULC types was the same: construction lands > unused lands > water > farmlands > grasslands > woodlands, meaning that the LULC type had an important influence on the $PM_{2.5}$ concentrations.

Effect of the LULCC type on $PM_{2.5}$. *LULCC matrix.* As showed in Table 3, in 2000, the main land type in Shanxi Province was farmland, whose area was 6.12×10^4 km^2, accounting for 39.09% of the total area. Next in total area were grasslands and woodlands, accounting for 29.16% and 28.01% respectively. Construction lands covered 0.42×10^4 km^2, accounting for 2.67% of the total area. The areas of water and unused lands were very little, accounting for just 0.97% and 0.10% respectively. In 2018, although farmlands still covered the largest area, its area reduced to 5.78×10^4 km^2, accounting for 36.91% of the total area. The area of woodlands increased, accounting for 28.36% of the total area, and became the second largest land type. The area of grasslands decreased by 0.16×10^4 km^2 and became the third largest land type. The area of construction lands increased dramatically, and its proportion increased to 5.56%, which was two times greater than in 2000. Water and unused lands still covered very little area, accounting for 0.94% and 0.08% of the total, respectively.

From the perspective of land being converting from one type to another, there was a large conversion of farmlands to other land types, roughly 2.29×10^4 km^2. Grasslands, woodlands, and construction lands underwent the largest amounts of change, accounting for 53.47%, 23.07%, and 20.91% of the total converted area, respectively. On the other hand, the other land types that were converted to farmlands accounted for 1.95×10^4 km^2, which significant decreased the total area of farmlands. The main conversion types of woodlands to other land types were grasslands, farmlands and construction lands. The sources of woodlands were mainly grasslands and farmlands. It was seen that the amount of woodlands converted to other types, and those converted to woodlands, were nearly equivalent in total area. Grasslands showed a similar trend as seen for the woodlands, which also showed a relatively stable state. Construction lands were mainly converted to farmlands, which accounted for 82.51% of the total converted area. The total area of construction lands that were converted to other types was 0.22×10^4 km^2. The main conversion sources of construction lands were farmlands, grasslands, and woodlands, and the total conversion area was 0.67×10^4 km^2, which was caused by fast urbanization.

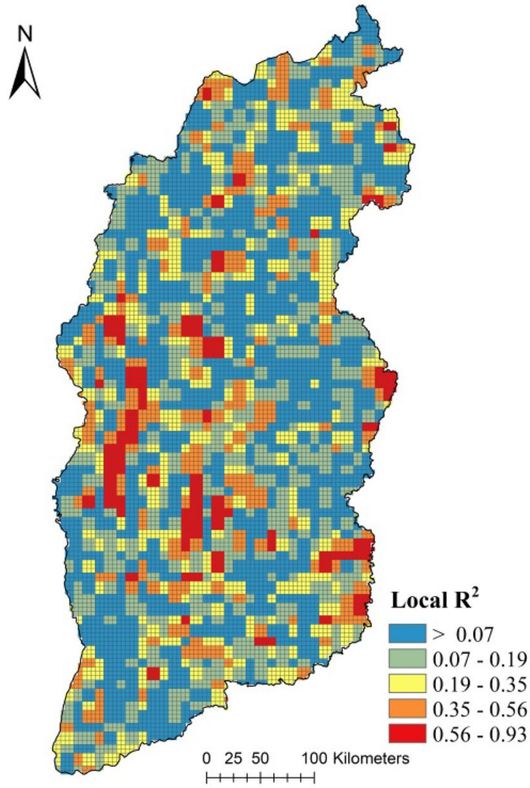

Figure 5. Local R^2 values from the GWR analysis.

LULC type	2000				2018			
	Min	Max	Mean	SD	Min	Max	Mean	SD
Farmlands	0	75.90	25.34	14.40	1.00	72.90	37.50	14.60
Woodlands	0	62.10	10.87	9.45	0.40	65.70	20.22	11.71
Grasslands	0	60.80	15.21	11.51	0.40	68.90	27.53	12.71
Water	0	72.30	29.78	16.04	1.80	73.10	41.23	15.16
Construction lands	0	75.60	33.92	13.58	1.70	74.40	43.95	14.45
Unused lands	0	68.50	30.21	14.92	2.50	63.80	43.45	14.11

Table 2. $PM_{2.5}$ concentrations of different the LULC types (units: μg/m^3).

2000	2018						Total
	Farmlands	Woodlands	Grasslands	Water	Construction lands	Unused lands	
Farmlands	38,293	5281	12,243	542	4788	41	61,188
Woodlands	4984	31,572	6572	118	584	8	43,838
Grasslands	12,058	7341	24,791	260	1162	25	45,637
Water	574	85	182	507	153	23	1524
Construction lands	1798	98	253	26	2005	4	4184
Unused lands	58	15	19	12	14	31	149
Total	57,765	44,392	44,060	1465	8706	132	156,520

Table 3. LULCC in Shanxi Province between 2000 and 2018 (units: km^2).

LULCC type	PM2.5 concentration		Reference variation range
	2000	2018	
Farmland to farmland	27.98	40.46	12.48
Woodland to woodland	10.16	18.79	8.63
Grassland to grassland	14.85	27.33	12.48
Construction land to construction land	35.58	50.67	15.09

Table 4. Dynamic $PM_{2.5}$ concentrations in the non-LULCC areas (units: μg/m^3).

LULCC type	PM2.5 concentration		Variation range	Reference variation range	Variation trend
	Before change	After change			
Farmland to woodland	15.58	26.11	10.53	12.48	− 1.94↓
Farmland to grassland	18.73	30.74	12.01	12.48	− 0.47↓
Farmland to construction land	31.30	45.52	14.22	12.48	1.74↑
Woodland to farmland	16.00	26.57	10.57	8.63	1.95↑
Woodland to grassland	9.69	21.99	12.30	8.63	3.68↑
Woodland to construction land	16.28	28.81	12.53	8.63	3.90↑
Grassland to farmland	18.76	31.48	12.26	12.48	0.24↑
Grassland to woodland	9.77	21.87	12.09	12.48	− 0.39↓
Grassland to construction land	18.82	33.82	15.01	12.48	2.52↑
Construction land to farmland	33.71	47.32	13.61	15.09	− 1.47↓
Construction land to woodland	20.31	34.48	14.18	15.09	− 0.91↓
Construction land to grassland	20.69	35.25	14.56	15.09	− 0.53↓

Table 5. Dynamic $PM_{2.5}$ concentrations in the LULCC areas (units: μg/m^3).

$PM_{2.5}$ dynamics. As water and unused lands covered only 1% of the total area, we only considered the other four land types (farmlands, woodlands, grasslands, and construction lands) to ascertain the influence of the LULCC types on the $PM_{2.5}$ dynamics. As discussed above, the $PM_{2.5}$ concentrations considerably increased from 2000 to 2018 for all land types, which indicated that there would be a $PM_{2.5}$ concentration increase for non-LULCC areas. The increase was mainly caused by increased pollution levels, not by LULCC. This would bring disturbance to our analysis. To avoid this disturbance, the range of $PM_{2.5}$ concentration variations in non-LULCC areas was calculated first (Table 4) and set as the reference variation range when analyzing the $PM_{2.5}$ concentration variations in the LULCC areas.

As showed in Table 4, the $PM_{2.5}$ dynamics in the different LULCC types showed two opposing trends, increasing and decreasing. The largest increase was for woodlands converted to construction lands, while the largest decline was for farmlands converted to woodlands. When farmlands were converted to woodlands and grasslands, the $PM_{2.5}$ concentrations declined, but when they were converted to construction lands, the $PM_{2.5}$ concentration increased. Increasing trends were seen when woodlands were converted to the other three land types. Conversely, declining trends were found when construction lands were converted to the other land types. When grasslands were converted to woodlands, a declining trend was witnessed, but when they were converted to the other two land types, increasing trends were seen.

As discussed above, the $PM_{2.5}$ concentrations for the four land types showed similar trends in both years: construction lands > farmlands > grasslands > woodlands. Therefore, according to the $PM_{2.5}$ concentrations, the four land types were divide into four grades: highest (construction lands), high (farmlands), medium (grasslands) and low (woodlands). As showed in Table 5, when high-grade land types are converted to low-grade types, the $PM_{2.5}$ concentrations decrease, and when low-grade land types are converted to high-grade types, the $PM_{2.5}$ concentrations increase.

Discussion

As an important energy base, the economic development of Shanxi Province has been mainly based on energy consumption, which continues to generate large quantities of harmful emissions[45]. Therefore, human activities were considered as the most important influence factor of $PM_{2.5}$ pollution[11]. However, LULC types were also representative of different human activities[46]. Different to previous studies, which mainly focused on discussing the relationship between land use type and $PM_{2.5}$ concentrations at urban scales[37,47], in this study we discussed the impact of land use on $PM_{2.5}$ concentrations from two aspects: different LULC and LULCC types at regional scales.

The different LULC types indicated the different intensities of human activities. Construction lands represented the highest intensity because of the high population density, traffic flow, industrial and commercial activities, etc., therein. All of these generate large quantities of air pollutants and caused the highest $PM_{2.5}$

concentrations[48]. Farmlands were also intensively affected by human activities, which caused relatively high $PM_{2.5}$ concentrations. Firstly, straw burning in farmlands can result in a sharp increase of $PM_{2.5}$ concentration within a short time[49]. Secondly, as a great agricultural country, the use of fertilizer in China is pervasive, and emissions arising from the manufacturing and use of fertilizer have a strong relationship with $PM_{2.5}$[50]. For example, fertilizer liberated from the soil can be converted into a precursor of $PM_{2.5}$[51]. Thirdly, heating activities in rural areas in winter mainly consist of burning coal, which generates large quantities of air pollutants and has an important impact on the $PM_{2.5}$ concentration in farmlands[52,53]. Vegetation covered area, including woodlands and grasslands, had relatively low $PM_{2.5}$ concentrations. These areas were less influenced by human activities, as indicated by the lower pollutant emissions therein. Meanwhile, it has been suggested that vegetation coverage has a negative regulating effect on $PM_{2.5}$ concentration[54,55]. Thus, woodlands have the lowest $PM_{2.5}$ concentrations because of their highest vegetation coverage.

The different LULCC types represented transitions among the different intensities of human activities, which caused dynamic changes of the $PM_{2.5}$ concentrations. When other land types were converted to construction lands, the intensity of human activities increased, which caused an increase of $PM_{2.5}$ concentration. A similar conclusion was found in another study, which showed that when natural land cover is replaced by manmade areas $PM_{2.5}$ concentrations increase[56]. Furthermore, other LULCC types were also discussed in our study. Farmlands may also contain intense human activities that can increase the $PM_{2.5}$ concentration, such as agricultural activities[57,58]. This was demonstrated by the increasing trend of $PM_{2.5}$ concentration when woodlands and grasslands were converted to farmlands. As vegetation coverage had a negative effect on $PM_{2.5}$ concentration[55], the $PM_{2.5}$ concentration also changed when the vegetation type changed; i.e. an increase trend was seen when woodlands were converted to grasslands.

Due to the limited LULC data, this study illustrated the influence of LULC and LULCC on $PM_{2.5}$ at the regional scale where human activities were considered as the most important influence factor. However, $PM_{2.5}$ pollution is both affected by human and natural factors[59]. In desert areas, natural factors including dust and wind could be the most important factors[60], while in coastal areas, climatic elements had the most important influence on $PM_{2.5}$ pollution[37]. These situations were not discussed in the present study. Future studies at larger scales are required to demonstrate the influence of LULC on $PM_{2.5}$ more comprehensively. The relationship between $PM_{2.5}$ pollution and its influence factors is complex and non-linear[61]. Traditional linear analysis methods have certain limitations and new non-linear analysis methods should be employed. Moreover, higher spatial and temporal resolution $PM_{2.5}$ data and LULC data are also required to better understand the response mechanism of $PM_{2.5}$ pollution to LULCC.

Conclusions

In this study, high-accuracy $PM_{2.5}$ data from ACAG and LULC data were employed to explore the relationship between $PM_{2.5}$ and LULCC. A GWR method was used for the general analysis, and a spatial analysis method based on the geographic information system was used for the detailed analysis. The main conclusions can be drawn as follows:

(1) The GWR analysis showed that R^2 reached 0.92, which represented a stable relationship between $PM_{2.5}$ and LULCC. High local R^2 values located in highly dynamic LULCC areas indicated that the dynamic $PM_{2.5}$ had a significant response to LULCC.

(2) In both considered years, 2000 and 2018, the order of $PM_{2.5}$ concentration in the different LULC types was the same: construction lands > unused lands > water > farmlands >grasslands > woodlands, meaning that the LULC type had an important influence on the $PM_{2.5}$ concentration.

(3) LULCC can also impact the dynamics of $PM_{2.5}$ concentration. When low-grade land types are converted to high-grade types, the $PM_{2.5}$ concentration increases; otherwise, it decreases. From another angle, when natural lands are converted to human-related lands, the $PM_{2.5}$ concentration increase; otherwise, the $PM_{2.5}$ concentrations decrease.

Received: 13 February 2021; Accepted: 17 August 2021
Published online: 02 September 2021

References

1. Ru-Jin, H. *et al.* High secondary aerosol contribution to particulate pollution during haze events in China. *Nature* **514**, 218–222 (2014).
2. Bilal, M., Nichol, J. E. & Spak, S. N. A new approach for estimation of fine particulate concentrations using satellite aerosol optical depth and binning of meteorological variables. *Aerosol Air Quality Res.* **17**, 356–367. https://doi.org/10.4209/aaqr.2016.03.0097 (2017).
3. Götschi, T., Heinrich, J., Sunyer, J. & Künzli, N. J. E. Long-term effects of ambient air pollution on lung function: A review. *Epidemiology* **19**, 690–701 (2008).
4. Jiang, Z., Kazuhiko, I., Ramona, L., Morton, L. & George, T. J. E. H. P. Time-series analysis of mortality effects of fine particulate matter components in Detroit and Seattle. *Environ. Health Perspect.* **119**, 461–466 (2011).
5. Weichenthal, *et al.* PM2.5, oxidant defence and cardiorespiratory health: a review. *Environ. Health* **12**, 40–40 (2013).
6. Cakmak, S. *et al.* Metal composition of fine particulate air pollution and acute changes in cardiorespiratory physiology. *Environ. Pollut.* **189**, 208–214 (2014).
7. Zhu, Y. *et al.* Indoor/outdoor relationships and diurnal/nocturnal variations in water-soluble ion and PAH concentrations in the atmospheric PM 2.5 of a business office area in Jinan, a heavily polluted city in China. *Atmos. Res.* **153**, 276–285 (2015).

8. Zhao, C. X., Wang, Y. Q., Wang, Y. J., Zhang, H. L. & Zhao, B. Q. J. E. S. Temporal and spatial distribution of PM_(2.5) and PM_(10) pollution status and the correlation of particulate matters and meteorological factors during Winter and Spring in Beijing. *Environ. Sci.* **35**, 418–427 (2014).
9. Guo, J. *et al.* Impact of diurnal variability and meteorological factors on the PM2.5—AOD relationship: Implications for PM2.5 remote sensing. *Environ. Pollut.* **221**, 94 (2017).
10. Hajiloo, F., Hamzeh, S. & Gheysari, M. Impact assessment of meteorological and environmental parameters on PM 2.5 concentrations using remote sensing data and GWR analysis (case study of Tehran). *Environ. Sci. Pollut. Res.* **26**, 24331–24345 (2018).
11. Bao, C. *et al.* Association of PM2.5 pollution with the pattern of human activity: A case study of a developed city in eastern China. *J. Air Waste Manag. Assoc.* **66**, 1202–1213 (2016).
12. Chan, C. K. & Yao, X. Air pollution in mega cities in China. *Atmos. Environ.* **42**, 1–42 (2008).
13. Kinney, P. L. *et al.* Traffic impacts on PM2.5 air quality in Nairobi, Kenya. *Environ. Sci. Policy* **14**, 369–378 (2011).
14. Jing, M., Liu, J., Yuan, X. & Shu, T. Tracing primary PM2.5 emissions via Chinese supply chains. *Environ. Res. Lett.* **10**, 054005 (2015).
15. Tao, C., He, J., Lu, X., She, J. & Guan, Z. Spatial and temporal variations of PM2.5 and its relation to meteorological factors in the urban area of Nanjing, China. *Int. J. Environ. Res. Public Health* **13**, 921 (2016).
16. Wang, Y., Qi, Y., Hu, J. & Zhang, H. Spatial and temporal variations of six criteria air pollutants in 31 provincial capital cities in China during 2013–2014. *Environ. Int.* **73**, 413–422 (2014).
17. Zhang, H., Wang, Z. & Zhang, W. Exploring spatiotemporal patterns of PM 2.5 in China based on ground-level observations for 190 cities. *Environ. Pollut.* **216**, 559–567 (2016).
18. Li, X. *et al.* The application of semicircular-buffer-based land use regression models incorporating wind direction in predicting quarterly NO_2 and PM 10 concentrations. *Atmos. Environ.* **103**, 18–24 (2015).
19. Li, L. *et al.* Spatial and temporal analysis of Air Pollution Index and its timescale-dependent relationship with meteorological factors in Guangzhou, China, 2001–2011. *Environ. Pollut.* **190**, 75–81 (2014).
20. Mazeikis, A. Urbanization influence on meteorological parameters of air pollution: Vilnius case study. *Baltica Int. J. Geosci.* **26**, 51–57 (2013).
21. Zhang, Y. L. & Cao, F. Fine particulate matter (PM 2.5) in China at a city level. *Sci. Rep.* **5**, 14884 (2015).
22. Wang, X., Wang, K. & Su, L. Contribution of atmospheric diffusion conditions to the recent improvement in air quality in China. *Sci. Rep.* **6**, 36404 (2016).
23. Bandeira, J. M., Coelho, M. C., Maria Elisa, S., Richard, T. & Carlos, B. Impact of land use on urban mobility patterns, emissions and air quality in a Portuguese medium-sized city. *Sci. Total Environ.* **409**, 1154–1163 (2011).
24. De, H. C. A regression-based method for mapping traffic-related air pollution: Application and testing in four contrasting urban environments. *Sci. Total Environ.* **253**, 151–167 (2000).
25. Liu, C., Henderson, B. H., Wang, D., Yang, X. & Peng, Z. R. A land use regression application into assessing spatial variation of intra-urban fine particulate matter (PM 2.5) and nitrogen dioxide (NO_2) concentrations in City of Shanghai, China. *Sci. Total Environ.* **565**, 607–615 (2016).
26. Yang, W. & Jiang, X. Interannual characteristics of fine particulate matter in North China and its relationship with land use and land cover change. *Environ. Sci.* **41**, 2995–3003 (2020).
27. Petit, C. C. & Lambin, E. F. Impact of data integration technique on historical land-use/land-cover change: Comparing historical maps with remote sensing data in the Belgian Ardennes. *Landsc. Ecol.* **17**, 117–132 (2002).
28. Zadbagher, E., Becek, K. & Berberoglu, S. Modeling land use/land cover change using remote sensing and geographic information systems: Case study of the Seyhan Basin, Turkey. *Environ. Monitor. Assess.* **190**, 494 (2018).
29. Sun, S. *et al.* Regulation of pollutant change and correlation analysis with vegetation index in Beijing–Tianjin–Hebei. *Environ. Sci.* https://doi.org/10.13227/j.hjkx.201809178 (2019).
30. Smith, R. L., Kolenikov, S. & Cox, L. H. Spatiotemporal modeling of PM2.5 data with missing values. *J. Geophys. Res. Atmos.* **108**, D24 (2003).
31. Chemel, C. *et al.* Application of chemical transport model CMAQ to policy decisions regarding PM2.5 in the UK. *Atmos. Environ.* **82**, 410–417 (2014).
32. Shi, Y., Lau, K. L. & Ng, E. Developing street-level PM2.5 and PM10 land use regression models in high-density Hong Kong with urban morphological factors. *Environ. Sci. Technol.* **50**, 8178–8187 (2016).
33. Xuefei, H. U. *et al.* Estimating ground-level PM2.5 concentrations in the Southeastern United States using MAIAC AOD retrievals and a two-stage model. *Remote Sens. Environ.* **140**, 220–232 (2014).
34. Van, D. A. *et al.* Global estimates of fine particulate matter using a combined geophysical–statistical method with information from satellites, models, and monitors. *Enviro. Sci. Technol.* **50**, 3762 (2016).
35. van Donkelaar, A., Martin, R. V., Li, C. & Burnett, R. T. Regional estimates of chemical composition of fine particulate matter using a combined geoscience-statistical method with information from satellites, models, and monitors. *Environ. Sci. Technol.* **53**, 2595–2611 (2019).
36. Yang, H., Chen, W., Liang, Z. J. I. J. O. E. R. & Health, P. Impact of land use on PM25 pollution in a representative city of middle China. *Int. J. Environ. Res. Public Health* **14**, 462 (2017).
37. Sun, L. *et al.* Impact of Land-Use and Land-Cover Change on urban air quality in representative cities of China. *J. Atmos. Solar-Terrest. Phys.* **142**, 43–54 (2016).
38. Yang, D. *et al.* Global distribution and evolvement of urbanization and PM2.5 (1998–2015). *Atmos. Environ.* **182**, 171–178 (2018).
39. Zheng, S. *et al.* The spatiotemporal distribution of air pollutants and their relationship with land-use patterns in Hangzhou city, China. *Atmosphere* **8**, 110 (2017).
40. Wu, J., Xie, W., Li, W. & Li, J. Effects of urban landscape pattern on PM2.5 pollution—a Beijing case study. *PloS one* **10**, e0142449 (2015).
41. Hammer, M. S., Donkelaar, A. V., Li, C., Lyapustin, A. & Martin, R. V. Global estimates and long-term trends of fine particulate matter concentrations (1998–2018). *Environ. Sci. Technol.* **54**, 7879–7890 (2020).
42. Propastin, P. Modifying geographically weighted regression for estimating aboveground biomass in tropical rainforests by multispectral remote sensing data. *Int. J. Appl. Earth Observ. Geoinform.* **18**, 82–90 (2012).
43. Jiang, M., Sun, W., Yang, G. & Zhang, D. Modelling seasonal GWR of daily PM2.5 with proper auxiliary variables for the Yangtze River Delta. *Remote Sens.* **9**, 346 (2017).
44. Xiya, Z. & Haibo, H. Spatio-temporal characteristics of aerosol optical depth and their relationship with urbanization over Beijing–Tianjin–Hebei Region. *Chin. J. Atmos. Sci.* **41**, 797–810 (2017).
45. Yang, W. & Jiang, X. Evaluating sustainable urbanization of resource-based cities based on the Mckinsey matrix: Case study in China. *J. Urban Plan. Dev.* **144**, 05017020 (2018).
46. Li, X. *et al.* A new global land-use and land-cover change product at a 1-km resolution for 2010 to 2100 based on human–environment interactions. *Ann. Am. Assoc. Geogr.* **107**, 1–20 (2017).
47. Li, J. & Huang, X. Impact of land-cover layout on particulate matter 2.5 in urban areas of China. *Int. J. Digit. Earth* **13**, 474–486 (2018).
48. Bismarck-Osten, C. V. *et al.* Characterization of parameters influencing the spatio-temporal variability of urban particle number size distributions in four European cities. *Atmos. Environ.* **77**, 415–429 (2013).

49. Zhang, L., Liu, Y. & Hao, L. J. E. R. L. Contributions of open crop straw burning emissions to PM2.5 concentrations in China. *Environ. Res. Lett.* **11**, 014014 (2016).
50. Pozzer, A. *et al.* Impact of agricultural emission reductions on fine-particulate matter and public health. *Atmos. Chem. Phys.* **17**, 1–19 (2017).
51. Han, L. *et al.* Meteorological and urban landscape factors on severe air pollution in Beijing. *J. Air Waste Manag. Assoc.* **65**, 782–787 (2015).
52. Fan, M., He, G. & Zhou, M. The winter choke: Coal-fired heating, air pollution, and mortality in China. *J. Health Econ.* **71**, 102316 (2020).
53. Xiao, Q., Ma, Z., Li, S. & Liu, Y. The impact of winter heating on air pollution in China. *PloS One* **10**, e0117311 (2015).
54. Yanan, L., Zhenming, D., Yuanjie, D., Mengyang, H. & Shunbo, Y. Relationship between urban industrialization and PM2.5 in China: Also discussing the internal mechanism of EKC. *Environ. Sci.* **41**, 1987–1996 (2020).
55. Tong, Z., Whitlow, T. H., Macrae, P. F., Landers, A. J. & Harada, Y. Quantifying the effect of vegetation on near-road air quality using brief campaigns. *Environ. Pollut.* **201**, 141–149 (2015).
56. Superczynski, S. D. & Christopher, S. A. Exploring land use and land cover effects on air quality in Central Alabama using GIS and remote sensing. *Remote Sens.* **3**, 2552–2567 (2011).
57. Zhang, H. *et al.* Emission characterization, environmental impact, and control measure of PM2.5 emitted from agricultural crop residue burning in China. *J. Clean. Prod.* **149**, 629–635 (2017).
58. Li, J. *et al.* Chemical characteristics and source apportionment of PM2.5 during the harvest season in eastern China's agricultural regions. *Atmos. Environ.* **92**, 442–448 (2014).
59. Yang, D. *et al.* Quantifying the influence of natural and socioeconomic factors and their interactive impact on PM2.5 pollution in China. *Environ. Pollut.* **241**, 475–483 (2018).
60. Xu, J., Zhou, G., Xu, Z. & De Zhou, S. Urban haze governance: Land use spatial conflict and governance urban air duct. *China Land Sci.* **29**, 49–56 (2015).
61. Lu, D., Mao, W., Xiao, W. & Zhang, L. Non-linear response of PM2.5 pollution to land use change in China. *Remote Sens.* **13**, 1612 (2021).

Acknowledgements

Funding for this study was obtained through the National Natural Science Foundation of China (No. 41701191), the Applied Basic Research Plan of Shanxi Province, China (No. 201701D221226) and the Science and Technology Innovation Project of Universities in Shanxi Province, China (No. 2019L0815). We are grateful to ACAG for providing the PM2.5 data used in this study. The authors also thank the reviewers for their valuable comments and suggestions.

Author contributions

W.Y. wrote the paper, X.J. processed the data.

Competing interests

The authors declare no competing interests.

Additional information

Correspondence and requests for materials should be addressed to W.Y.

Reprints and permissions information is available at www.nature.com/reprints.

Publisher's note Springer Nature remains neutral with regard to jurisdictional claims in published maps and institutional affiliations.